Spin-mixing conductances of metallic and half-metallic magnetic layers

2007 J. Phys.: Condens. Matter 19 365203

(http://iopscience.iop.org/0953-8984/19/36/365203)

IOP PUBLISHING JOURNAL OF PHYSICS: CONDENSED MATTER

J. Phys.: Condens. Matter **19** (2007) 365203 (11pp) doi:10.1088/0953-8984/19/36/365203

Spin-mixing conductances of metallic and half-metallic magnetic layers

I Turek[1] **and K Carva**[2]

[1] Institute of Physics of Materials, Academy of Sciences of the Czech Republic, Žižkova 22, CZ-61662 Brno, Czech Republic
[2] Department of Condensed Matter Physics, Faculty of Mathematics and Physics, Charles University, Ke Karlovu 5, CZ-12116 Prague 2, Czech Republic

E-mail: turek@ipm.cz and carva@karlov.mff.cuni.cz

Received 28 November 2006
Published 24 August 2007
Online at stacks.iop.org/JPhysCM/19/365203

Abstract

The spin-mixing conductance of a thin ferromagnetic layer attached epitaxially to two semi-infinite non-magnetic metallic leads is formulated in terms of non-equilibrium Green's functions. The spin-mixing conductance is obtained as a response of the spin torque acting on the ferromagnet with respect to the spin accumulation in one of the leads, while the spin torque is defined as a time derivative of the spin magnetic moment. The equivalence of the derived formula with a previous expression of the Landauer–Büttiker scattering theory is sketched and an implementation within the *ab initio* tight-binding linear muffin-tin orbital method is briefly described. Applications are made for metallic Co- and Ni-based slabs embedded between Cu(111) leads and for half-metallic Co_2MnSi films sandwiched by Cr(001) leads. The calculated results throw serious doubts on the general validity of two features: fast convergence of the spin-mixing conductance with increasing thickness of the magnetic layer and negligible values of the imaginary part of the spin-mixing conductance as compared to the real part.

1. Introduction

Artificially prepared metallic magnetic multilayers and spin valves attract ongoing interest due to a unique interplay between their magnetic structure and transport properties [1, 2], especially in the current perpendicular to the planes (CPP) geometry. This was manifested by the well-known giant magnetoresistance effect [3] and by more recent investigations of current-induced magnetization switching [4–7].

Probably the most successful phenomenological framework for quantitative understanding of both phenomena is the Valet–Fert model [8], based on the linearized Boltzmann equation. The description of the CPP transport in collinear spin structures within this scheme leads to a semiclassical concept of the spin accumulation in non-magnetic layers, i.e., to a difference of effective chemical potentials (Fermi levels) for electrons in the two spin channels. A recent

generalization of the Valet–Fert model to non-collinear spin structures [9–11] employs two properties of spin currents. First, the transverse (perpendicular to the local exchange field) component of the spin current inside a ferromagnet becomes rapidly damped over a typical distance of a few interatomic spacings [12]. This very short magnetic coherence length is the result of a large exchange splitting which leads to mostly destructive interference effects due to all contributions of wavevectors on the two Fermi surfaces of the ferromagnetic metal. Consequently, the spin torque experienced by a ferromagnetic (FM) layer can be identified with the transverse spin current at its interface with a neighbouring non-magnetic (NM) layer. Second, the proper boundary conditions that are inevitable for a full solution of the diffusion equations must be formulated in terms of spin-mixing conductances of individual interfaces [13]. The latter (complex) quantities together with the spin-resolved interface conductances provide complete information on a linear response of the currents and spin currents at an interface due to the bias and the spin accumulation deep inside the adjacent materials. The spin-mixing conductances are indispensable also for the magnetoelectronic circuit theory of non-collinear magnetic systems [13–15].

Several authors have addressed the properties of a single NM/FM interface [12, 16], with emphasis put on the conductances and their sensitivity, e.g., to interface alloying. Since the traditional Landauer–Büttiker scattering theory [17] has been used in the majority of papers, the effect of disorder was included by a supercell technique [15, 18].

The spin-mixing conductances of FM layers of a finite thickness attached to two NM leads have been studied very recently for Co/Cu, Fe/Au and Fe/Cr systems [19]. It has been found that the thickness dependence of the real part of the spin-mixing conductance saturates very rapidly for thicker layers; this behaviour is equivalent to the very short magnetic coherence length, and it proves that the spin-mixing conductance is predominantly an interface property. However, this may not hold for other ferromagnets, such as Ni and Ni-based alloys or the diluted magnetic semiconductors (Ga, Mn)As [10], where the average exchange splitting is rather weak. For systems investigated so far, the imaginary part of the spin-mixing conductance was found to be appreciably smaller than the real part [16, 19]. This property has been employed as an assumption in a number of theoretical studies [9, 10, 19, 20]; its validity, however, has to be checked in each particular case.

The present paper serves two main purposes. First, we consider an FM layer embedded between two NM metallic leads with epitaxial interfaces and give a general theoretical formulation of the spin torque due to the spin accumulation in one of the leads (section 2.1). We use the language of non-equilibrium Green's functions (NGFs) [17, 21] as an alternative to the scattering theory. We also briefly describe a numerical implementation within the first-principles tight-binding linear muffin-tin orbital (TB-LMTO) method [22, 23] (section 2.2). The method has recently been combined with the coherent potential approximation (CPA) [23–25] for the collinear CPP transport in disordered multilayers [26], and we employ the same configuration averaging here. Second, we perform calculations for systems based on pure elemental metals (Cu, Co, Ni) including a random binary alloy $Ni_{0.84}Fe_{0.16}$ (permalloy, Py) (section 3.1). We also report the results for slabs of a half-metallic ferromagnet Co_2MnSi (section 3.2) and interpret them in terms of a free-electron model of an interface between an NM metal and an FM half-metal (section 3.3).

2. Theory

2.1. General formulation of the spin-mixing conductance

We consider an NM/FM/NM system with non-interacting electrons. Its effective one-electron Hamiltonian H can be written as

$$H = H_0 + \gamma(\boldsymbol{\sigma} \cdot \boldsymbol{n}), \tag{1}$$

where H_0 represents a spin-independent part, γ is the exchange splitting, which is non-zero only inside an intermediate region containing the FM layer and narrow parts of the two adjacent semi-infinite NM leads, the vector $\boldsymbol{\sigma} = (\sigma_x, \sigma_y, \sigma_z)$ denotes a vector of the Pauli matrices, and the unit vector $\boldsymbol{n}$ defines the direction of the exchange field of the FM layer. The spin dependence of the Hamiltonian H in (1) implies that electrons with spin parallel and antiparallel to $\boldsymbol{n}$ experience Hamiltonians $H_\uparrow = H_0 + \gamma$ and $H_\downarrow = H_0 - \gamma$, respectively.

We define the spin torque $\boldsymbol{\tau}$ as the time derivative of the total spin magnetic moment. The latter operator is represented by the Pauli matrices $\boldsymbol{\sigma}$, so that

$$\boldsymbol{\tau} = -\mathrm{i}[\boldsymbol{\sigma}, H], \tag{2}$$

where atomic units ($\hbar = 1$) are used. Note that this definition of the spin torque is formally different from (but physically equivalent to) the formulation based on spin currents on both sides of the FM layer [4, 27]. The well-known algebraic rules for the Pauli matrices yield an explicit form of the torque operator

$$\boldsymbol{\tau} = 2\gamma \boldsymbol{n} \times \boldsymbol{\sigma}, \tag{3}$$

which shows that $\boldsymbol{\tau}$ is a local operator that is non-zero only inside the intermediate region; its direction is perpendicular to the FM exchange field.

The thermodynamic average of the spin torque $\boldsymbol{\tau}$ for the NM/FM/NM system in a stationary non-equilibrium state is given by [17, 21]

$$\bar{\boldsymbol{\tau}} = \frac{1}{2\pi} \int_{-\infty}^{\infty} \mathrm{Tr}\{\boldsymbol{\tau} G^<(E)\}\, \mathrm{d}E, \tag{4}$$

where $G^<(E)$ is the lesser component of the non-equilibrium Green's function. The latter quantity is related to the retarded and the advanced Green's functions, $G^\mathrm{r}(E)$ and $G^\mathrm{a}(E)$, respectively, by means of

$$G^<(E) = G^\mathrm{r}(E)\Sigma^<(E)G^\mathrm{a}(E), \qquad G^{\mathrm{r,a}}(E) = [E - H - \Sigma^{\mathrm{r,a}}(E)]^{-1}, \tag{5}$$

where $\Sigma^<(E)$, $\Sigma^\mathrm{r}(E)$ and $\Sigma^\mathrm{a}(E)$ denote the lesser, the retarded and the advanced components of the selfenergy, respectively. Note that all operators in (4) and (5) are defined in the Hilbert space of the intermediate region.

The spin accumulation in the NM leads results in a change of the lesser selfenergy $\delta\Sigma^<(E)$ (see below) which induces a first-order change of the average torque (4):

$$\delta\bar{\boldsymbol{\tau}} = \frac{1}{2\pi} \int_{-\infty}^{\infty} \mathrm{Tr}\{G^\mathrm{a}(E)\boldsymbol{\tau} G^\mathrm{r}(E)\delta\Sigma^<(E)\}\, \mathrm{d}E. \tag{6}$$

The special form of the torque operator (2) together with the expression for $G^{\mathrm{r,a}}(E)$ (5) provide a relation

$$G^\mathrm{a}(E)\boldsymbol{\tau} G^\mathrm{r}(E) = -\mathrm{i}[\boldsymbol{\sigma} G^\mathrm{r}(E) - G^\mathrm{a}(E)\boldsymbol{\sigma}] + G^\mathrm{a}(E)\boldsymbol{\sigma}\Gamma(E)G^\mathrm{r}(E), \tag{7}$$

where we have introduced an abbreviation for the antiHermitean part of the selfenergy, namely

$$\Gamma(E) = \mathrm{i}[\Sigma^\mathrm{r}(E) - \Sigma^\mathrm{a}(E)]. \tag{8}$$

In deriving (7), use was made of the fact that the selfenergies of the unperturbed NM leads are spin-independent, so that $[\boldsymbol{\sigma}, \Sigma^{\mathrm{r,a}}(E)] = 0$.

The total selfenergies can be written as sums of separate contributions due to the left ($\mathcal{L}$) and the right ($\mathcal{R}$) leads,

$$\Sigma^<(E) = \Sigma^<_\mathcal{L}(E) + \Sigma^<_\mathcal{R}(E), \qquad \Sigma^{\mathrm{r,a}}(E) = \Sigma^{\mathrm{r,a}}_\mathcal{L}(E) + \Sigma^{\mathrm{r,a}}_\mathcal{R}(E). \tag{9}$$

For stationary non-equilibrium systems without spin accumulation, the lesser selfenergies are given by

$$\Sigma^{<}_{\mathcal{L},\mathcal{R}}(E) = f_{\mathcal{L},\mathcal{R}}(E)\Gamma_{\mathcal{L},\mathcal{R}}(E), \qquad \Gamma_{\mathcal{L},\mathcal{R}}(E) = \mathrm{i}[\Sigma^{\mathrm{r}}_{\mathcal{L},\mathcal{R}}(E) - \Sigma^{\mathrm{a}}_{\mathcal{L},\mathcal{R}}(E)], \tag{10}$$

where the functions $f_{\mathcal{L},\mathcal{R}}(E)$ refer to the Fermi–Dirac distributions of the two leads. Note that $\Gamma(E) = \Gamma_{\mathcal{L}}(E) + \Gamma_{\mathcal{R}}(E)$.

In the thermodynamic equilibrium, the distributions $f_{\mathcal{L},\mathcal{R}}(E)$ coincide with the Fermi–Dirac distribution of the whole system. In the presence of spin accumulation in one of the leads ($\mathcal{L}$), the system is driven out of equilibrium by adding a spin-dependent shift $\delta E_{\mathcal{L}}$ to the Fermi energy of the lead. This yields the first-order change of $\Sigma^{<}(E)$:

$$\delta\Sigma^{<}(E) = \delta\Sigma^{<}_{\mathcal{L}}(E) = f'(E)(\boldsymbol{\sigma}\cdot\boldsymbol{a})\Gamma_{\mathcal{L}}(E)\delta E_{\mathcal{L}}, \tag{11}$$

where $f'(E)$ means the derivative of the Fermi–Dirac distribution and $\boldsymbol{a}$ is a unit vector pointing in the direction of the spin accumulation. For systems at zero temperature, which will be considered in the following, $f'(E) = -\delta(E - E_{\mathrm{F}})$, where E_{F} is the Fermi energy. Substitution of (7) and (11) into (6) provides a starting expression for the corresponding response coefficient $\boldsymbol{C}_{\mathcal{L}}$:

$$\boldsymbol{C}_{\mathcal{L}} \equiv \frac{\delta\bar{\boldsymbol{\tau}}}{\delta E_{\mathcal{L}}} = \frac{1}{2\pi}\,\mathrm{Tr}[\mathrm{i}(\boldsymbol{\sigma}G^{\mathrm{r}} - G^{\mathrm{a}}\boldsymbol{\sigma})(\boldsymbol{\sigma}\cdot\boldsymbol{a})\Gamma_{\mathcal{L}} - \boldsymbol{\sigma}\Gamma G^{\mathrm{r}}(\boldsymbol{\sigma}\cdot\boldsymbol{a})\Gamma_{\mathcal{L}}G^{\mathrm{a}}], \tag{12}$$

where all omitted energy arguments equal the Fermi energy E_{F}.

In order to extract the dependence of the response coefficient $\boldsymbol{C}_{\mathcal{L}}$ on the orientation of the spin accumulation $\boldsymbol{a}$ and the magnetization direction $\boldsymbol{n}$, the explicit structure of the Green's functions $G^{\mathrm{r,a}}$ of the Hamiltonian (1) with respect to the spin must be used,

$$G^{\mathrm{r,a}} = \frac{G^{\mathrm{r,a}}_{\uparrow} + G^{\mathrm{r,a}}_{\downarrow}}{2} + \frac{G^{\mathrm{r,a}}_{\uparrow} - G^{\mathrm{r,a}}_{\downarrow}}{2}(\boldsymbol{\sigma}\cdot\boldsymbol{n}), \tag{13}$$

where the spin-resolved Green's functions are defined by

$$G^{\mathrm{r,a}}_{s}(E) = [E - H_s - \Sigma^{\mathrm{r,a}}(E)]^{-1}, \qquad s = \uparrow, \downarrow . \tag{14}$$

The substitution of (13) into (12) reduces its right-hand side to a sum of terms of the form $\mathrm{Tr}(\xi X) = \mathrm{tr_S}(\xi)\,\mathrm{tr}(X)$, where ξ is a matrix in the spin indices only while X is a matrix in the other (site and orbital) indices and where the symbols $\mathrm{tr_S}$ and tr denote the respective trace operations. Further steps employ trace relations:

$$\begin{aligned} &\mathrm{tr_S}[\boldsymbol{\sigma}(\boldsymbol{\sigma}\cdot\boldsymbol{a})] = 2\boldsymbol{a}, \qquad \mathrm{tr_S}[\boldsymbol{\sigma}(\boldsymbol{\sigma}\cdot\boldsymbol{n})(\boldsymbol{\sigma}\cdot\boldsymbol{a})] = 2\mathrm{i}\boldsymbol{n}\times\boldsymbol{a}, \\ &\mathrm{tr_S}[\boldsymbol{\sigma}(\boldsymbol{\sigma}\cdot\boldsymbol{n})(\boldsymbol{\sigma}\cdot\boldsymbol{a})(\boldsymbol{\sigma}\cdot\boldsymbol{n})] = 4(\boldsymbol{n}\cdot\boldsymbol{a})\boldsymbol{n} - 2\boldsymbol{a}. \end{aligned} \tag{15}$$

The resulting expression for $\boldsymbol{C}_{\mathcal{L}}$ follows after a lengthy but straightforward manipulation:

$$\boldsymbol{C}_{\mathcal{L}} = D_1\boldsymbol{a} + D_2\boldsymbol{a}\times\boldsymbol{n} - D_3(\boldsymbol{n}\cdot\boldsymbol{a})\boldsymbol{n}, \tag{16}$$

where the prefactors D_1, D_2 and D_3 are given by

$$\begin{aligned} D_1 &= \frac{1}{2\pi}\,\mathrm{tr}[\mathrm{i}(G^{\mathrm{r}}_{\uparrow} + G^{\mathrm{r}}_{\downarrow} - G^{\mathrm{a}}_{\uparrow} - G^{\mathrm{a}}_{\downarrow})\Gamma_{\mathcal{L}} - \Gamma G^{\mathrm{r}}_{\uparrow}\Gamma_{\mathcal{L}}G^{\mathrm{a}}_{\downarrow} - \Gamma G^{\mathrm{r}}_{\downarrow}\Gamma_{\mathcal{L}}G^{\mathrm{a}}_{\uparrow}], \\ D_2 &= \frac{1}{2\pi}\,\mathrm{tr}[(G^{\mathrm{r}}_{\uparrow} - G^{\mathrm{r}}_{\downarrow} + G^{\mathrm{a}}_{\uparrow} - G^{\mathrm{a}}_{\downarrow})\Gamma_{\mathcal{L}} + \mathrm{i}(\Gamma G^{\mathrm{r}}_{\uparrow}\Gamma_{\mathcal{L}}G^{\mathrm{a}}_{\downarrow} - \Gamma G^{\mathrm{r}}_{\downarrow}\Gamma_{\mathcal{L}}G^{\mathrm{a}}_{\uparrow})], \\ D_3 &= \frac{1}{2\pi}\,\mathrm{tr}[\Gamma(G^{\mathrm{r}}_{\uparrow} - G^{\mathrm{r}}_{\downarrow})\Gamma_{\mathcal{L}}(G^{\mathrm{a}}_{\uparrow} - G^{\mathrm{a}}_{\downarrow})]. \end{aligned} \tag{17}$$

The form of (16) can be simplified by using a general relation

$$\mathrm{i}[G^{\mathrm{r}}(E) - G^{\mathrm{a}}(E)] = G^{\mathrm{a}}(E)\Gamma(E)G^{\mathrm{r}}(E) \tag{18}$$

that follows from (5) and (8). After inserting the spin-resolved counterparts of (18), $\mathrm{i}(G_s^{\mathrm{r}} - G_s^{\mathrm{a}}) = G_s^{\mathrm{a}}\Gamma G_s^{\mathrm{r}}$ ($s = \uparrow, \downarrow$), in the expression (17) for D_1, one obtains $D_3 = D_1$. The previous formula (16) for the response coefficient $\boldsymbol{C}_{\mathcal{L}}$ can thus be rewritten as

$$\boldsymbol{C}_{\mathcal{L}} = D_1 \boldsymbol{n} \times (\boldsymbol{a} \times \boldsymbol{n}) + D_2 \boldsymbol{a} \times \boldsymbol{n}, \tag{19}$$

i.e., in a form explicitly perpendicular to the vector $\boldsymbol{n}$; see the text after (3).

A closer inspection of the real quantities D_1 and D_2 (17) reveals their simple relation to a single complex quantity—the spin-mixing conductance $C_{\mathcal{L}}^{\mathrm{mix}}$:

$$C_{\mathcal{L}}^{\mathrm{mix}} = \frac{1}{2\pi}\,\mathrm{tr}[\mathrm{i}(G_{\uparrow}^{\mathrm{r}} - G_{\downarrow}^{\mathrm{a}})\Gamma_{\mathcal{L}} - \Gamma G_{\uparrow}^{\mathrm{r}}\Gamma_{\mathcal{L}} G_{\downarrow}^{\mathrm{a}}], \tag{20}$$

which yields

$$D_1 = 2\,\mathrm{Re}\,C_{\mathcal{L}}^{\mathrm{mix}}, \qquad D_2 = 2\,\mathrm{Im}\,C_{\mathcal{L}}^{\mathrm{mix}}. \tag{21}$$

Note that the usual spin-resolved charge conductances (in units of $e^2/\hbar$) are given by

$$C_s = \frac{1}{2\pi}\,\mathrm{tr}(\Gamma_{\mathcal{R}} G_s^{\mathrm{r}} \Gamma_{\mathcal{L}} G_s^{\mathrm{a}}), \qquad s = \uparrow, \downarrow\,. \tag{22}$$

The real part of $C_{\mathcal{L}}^{\mathrm{mix}}$ is positive, as can be shown from its relation to the prefactor D_3, see (17) and the text after (18), and from the positive definiteness of the operators $\Gamma_{\mathcal{L},\mathcal{R}}$. The formulae (19)–(21) represent the central result of this section.

The derived dependence of the spin torque (19) on the orientation of the unit vectors $\boldsymbol{a}$ and $\boldsymbol{n}$ is identical to that obtained within the Landauer–Büttiker theory [15]. In order to compare the latter to the NGF approach more explicitly, let us consider the simplest case of a one-dimensional NM/FM/NM system with one propagating mode in identical NM leads. It can be shown that the spin-resolved charge conductances (22) for this system are equal to $C_s = |t_s|^2/(2\pi)$, while the spin-mixing conductance (20) is given by

$$C_{\mathcal{L}}^{\mathrm{mix}} = \frac{1}{2\pi}(1 - r_{\uparrow} r_{\downarrow}^{*}) - \frac{1}{2\pi} t_{\uparrow} t_{\downarrow}^{*}, \tag{23}$$

where t_s and r_s denote respectively the spin-resolved transmission and reflection coefficients of the wave incoming from the left lead. This result proves an equivalence of the developed NGF approach and the Landauer–Büttiker formalism [15]. In particular, the first term in (23) was identified with the spin-mixing conductance of a single NM/FM interface [13, 14, 16] while the second term due to the transmitted electrons appeared naturally for FM layers of a finite thickness [15, 19, 20, 27, 28]. The possible presence of several propagating modes in the leads can be taken into account by double summations over these channels in (23), as explained in detail in [14, 15, 19].

2.2. *Implementation and computational details*

The formalism of section 2.1 is well suited for implementation within the *ab initio* TB-LMTO method in the atomic sphere approximation [22, 23, 29]. Since details of this technique including calculations of the transport properties have recently been described in the literature [26, 30–33], we display here only the final TB-LMTO formula for the spin-mixing conductance $C_{\mathcal{L}}^{\mathrm{mix}}$ (20). Its value per two-dimensional (2D) unit cell of an epitaxial NM/FM/NM system is given by

$$C_{\mathcal{L}}^{\mathrm{mix}} = \frac{1}{2\pi}\frac{1}{N_{\parallel}}\,\mathrm{tr}[\mathrm{i}(g_{\uparrow}^{\mathrm{r}} - g_{\downarrow}^{\mathrm{a}})\mathcal{B}_{\mathcal{L}} - (\mathcal{B}_{\mathcal{L}} + \mathcal{B}_{\mathcal{R}}) g_{\uparrow}^{\mathrm{r}} \mathcal{B}_{\mathcal{L}} g_{\downarrow}^{\mathrm{a}}], \tag{24}$$

where $N_{\parallel}$ refers to a large number of 2D cells in directions parallel to atomic layers and the trace is taken over the site and the orbital indices of the intermediate region. The quantities g_s^{r} and g_s^{a}

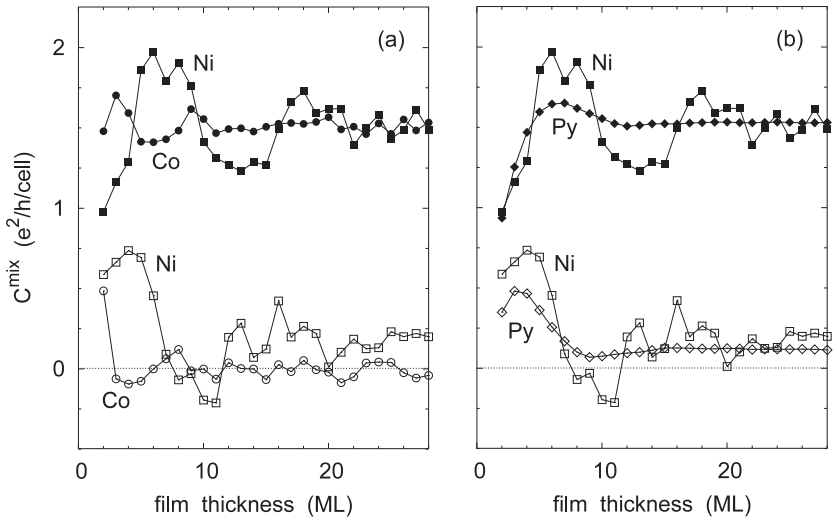

Figure 1. Spin-mixing conductances $C^{\mathrm{mix}}_{\mathcal{L}}$ of fcc(111) systems as functions of the magnetic film thickness: (a) Cu/Ni/Cu (■, □) and Cu/Co/Cu (●, ○), and (b) Cu/Ni/Cu (■, □) and Cu/Py/Cu (◆, ◇). The filled and the empty symbols denote respectively the real and the imaginary parts of $C^{\mathrm{mix}}_{\mathcal{L}}$.

($s = \uparrow, \downarrow$) denote spin-resolved auxiliary Green's function matrices calculated respectively at energies $E_{\mathrm{F}} + \mathrm{i}\eta$ and $E_{\mathrm{F}} - \mathrm{i}\eta$, where $\eta \to 0^+$. The spin-independent matrices $\mathcal{B}_{\mathcal{L},\mathcal{R}}$ correspond to antiHermitean parts of selfenergies of the NM leads [26, 30]. In the principal-layer technique employed here, the intermediate region consists of N principal layers and the matrices $\mathcal{B}_{\mathcal{L}}$ and $\mathcal{B}_{\mathcal{R}}$ are localized in the first and in the Nth principal layer, respectively.

For epitaxial systems with perfect 2D translational symmetry, the evaluation of (24) rests on the lattice Fourier transformation of the involved matrices. For FM layers with substitutional disorder, attached to non-random NM leads, the CPA is used for configurational averaging [23, 29]. The CPA-vertex corrections due to the second term in (24) are formulated and calculated according to [26].

The systems studied in section 3 were based on face-centred cubic (fcc) and body-centred cubic (bcc) lattices with neglected lattice relaxations. One principal layer was formed by one atomic layer for fcc(111) stacking (section 3.1) while two neighbouring atomic layers per principal layer were taken for bcc(001) stacking (section 3.2). The imaginary parts of energies for conductance calculations were set $\eta = 10^{-7}$ Ryd while evaluation of the trace in (24) employed $\mathbf{k}_{\parallel}$-mesh densities equivalent to 5000 sampling points in a 2D Brillouin zone of the 1×1 unit cell of the NM leads.

3. Results and discussion

3.1. Co- and Ni-based metallic layers attached to Cu(111) leads

The calculated spin-mixing conductances of Cu/Co/Cu(111), Cu/Ni/Cu(111) and Cu/Py/Cu(111) systems are shown in figure 1 as functions of the thickness (in monolayers, ML) of the magnetic films. The values and the trends of $C^{\mathrm{mix}}_{\mathcal{L}}$ for the Cu/Co/Cu system (figure 1(a)) are in reasonable agreement with results of a previous study [19]: the thickness dependence exhibits small oscillations that however decay rapidly with increasing Co thickness,

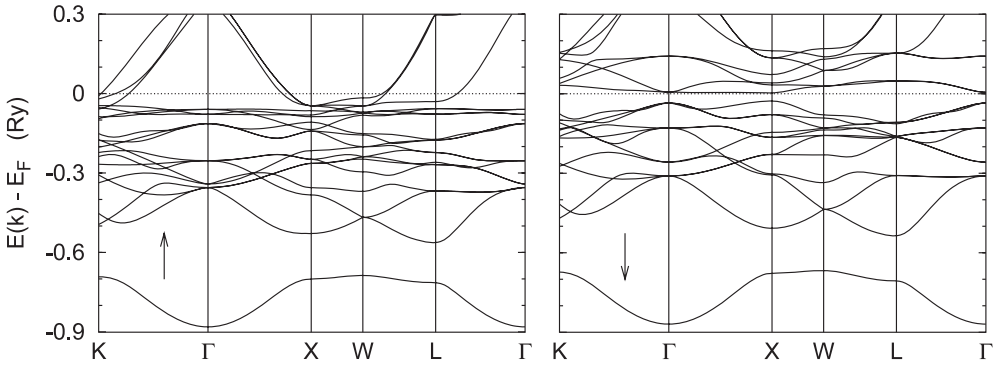

Figure 2. Band structure of the full-Heusler compound Co_2MnSi in the spin-↑ (left panel) and the spin-↓ (right panel) channels.

and the imaginary part of $C_{\mathcal{L}}^{\mathrm{mix}}$ is at least an order of magnitude smaller than the real part; the only exception represents the thinnest Co film (2 ML) considered. This behaviour is typical for metallic ferromagnets with a strong exchange splitting which leads to large differences between the spin-↑ and spin-↓ Fermi surfaces and to cancellation of phase factors for different $\mathbf{k}_{\parallel}$-vectors [15, 19].

The oscillations of $C_{\mathcal{L}}^{\mathrm{mix}}$ in the Cu/Ni/Cu system have bigger amplitudes and a slower decay with increasing Ni thickness as compared to the Cu/Co/Cu case (figure 1(a)). This behaviour can be ascribed to different magnitudes of the exchange splitting: that of Ni is significantly smaller than that of Co. Since these oscillations arise due to quantum interference effects, they can be strongly reduced by impurities in the FM film. This is documented by spin-mixing conductances of the Cu/Py/Cu system (figure 1(b)): the random Fe atoms suppress any long-range oscillations and the asymptotic value of $C_{\mathcal{L}}^{\mathrm{mix}}$ is achieved practically for Py thickness of 10 ML.

3.2. Half-metallic Co_2MnSi layers attached to Cr(001) leads

The ferromagnetic full-Heusler compound Co_2MnSi with the $L2_1$ structure represents a promising material for spintronics applications due to its high Curie temperature of 985 K [34] and due to recent predictions [35, 36] and experimental verification [37] of its half-metallic nature.

The self-consistent electronic structure of bulk Co_2MnSi, calculated by means of the TB-LMTO method for an experimental value of the fcc lattice parameter [34], is presented in figures 2 and 3. The narrow band gap in the spin-↓ channel (figure 2) is 0.43 eV wide, and the alloy Fermi energy E_{F} is located only 0.05 eV below the conduction band, in rough agreement with measurements indicating the width of the band gap of 0.35–0.40 eV and a tiny separation of 0.01 eV between the E_{F} and the bottom of the conduction band [37]. The shape of the spin-polarized densities of states (figure 3) and the total spin moment of 5 μ_{B} per formula unit agree well with previous full-potential calculations [36].

The CPP transport properties were studied for (001) slabs of the Co_2MnSi compound sandwiched by non-magnetic Cr bcc(001) leads, as motivated by an epitaxially prepared Cr/Co_2MnSi interface [37]. All atoms were placed at sites of an ideal bcc lattice which required a small (∼2%) compression inside the Cr leads as compared to an equilibrium Cr bcc structure. The Co_2MnSi slabs comprised an even number of atomic layers; the pure Co-layer and the MnSi-layer were adjacent to the left and the right Cr lead, respectively.

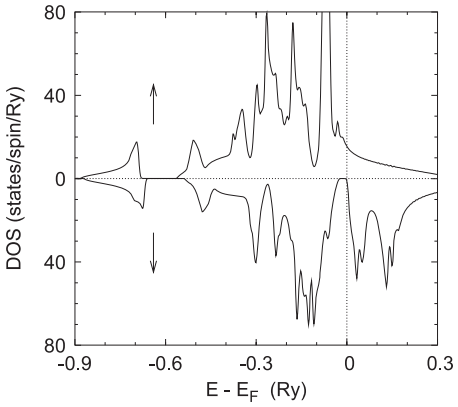

Figure 3. Spin-resolved densities of states (per formula unit) of the bulk full-Heusler compound Co_2MnSi.

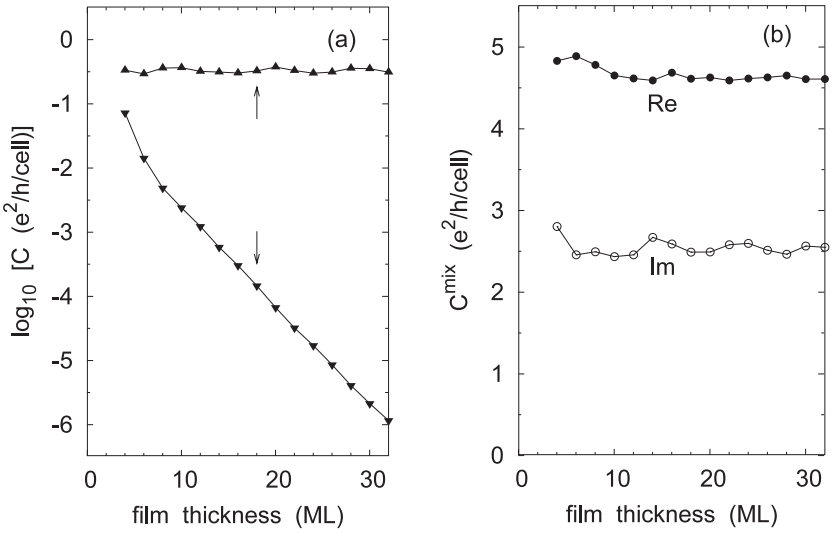

Figure 4. Transport properties of $Cr/Co_2MnSi/Cr(001)$ as functions of the Co_2MnSi thickness: (a) the spin-↑ (▲) and the spin-↓ (▼) conductances, and (b) the real (●) and the imaginary (○) parts of the spin-mixing conductance.

The calculated transport properties are summarized in figure 4 as functions of the Co_2MnSi thickness. The spin-resolved conductances (figure 4(a)) reflect a metallic regime in the spin-↑ channel, whereas a tunnelling regime is clearly observed in the spin-↓ channel. Note that a full spin polarization of the current is obtained very quickly with increasing Co_2MnSi thickness, despite the small energy separation between the Fermi energy and the bottom edge of the spin-↓ conduction band in the bulk compound.

The thickness dependence of the spin-mixing conductance (figure 4(b)) exhibits a nearly constant value with superimposed small oscillations due to quantum-size effects, in analogy to the case of a metallic FM film with a strong exchange splitting, such as Cu/Co/Cu(111) (section 3.1). However, the imaginary part of $C_{\mathcal{L}}^{\mathrm{mix}}$ acquires values as high as one half of the real part in the case of $Cr/Co_2MnSi/Cr(001)$. Such a high value of the imaginary part of

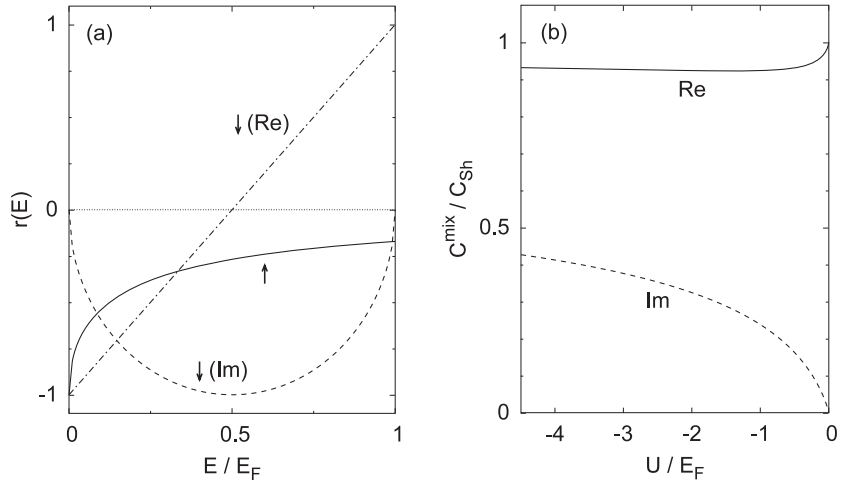

Figure 5. Free-electron model of an interface between a non-magnetic metal and a half-metallic ferromagnet: (a) energy-dependent reflection coefficients in the spin-↑ channel for the potential $U = -E_F$ (——) and in the spin-↓ channel (real part, — · —, and imaginary part, - - - -), and (b) the spin-mixing conductance as a function of the spin-↑ potential U (real part, ——, and imaginary part, - - - -).

the spin-mixing conductance has not been encountered in metallic NM/FM and NM/FM/NM systems [15, 16, 19]; this new feature thus calls for an explanation based on the underlying electronic structure.

3.3. Spin-mixing conductances in a free-electron model

In order to explain the unexpected properties of the spin-mixing conductance in presence of a half-metallic FM film qualitatively, let us consider the simplest free-electron model of the NM/FM/NM system that was used by several authors in the past [12, 19]. Since the spin-↓ channel is in a tunnelling regime, the transmitted electrons contribute negligibly to $C_{\mathcal{L}}^{\mathrm{mix}}$, and we can thus reduce the problem to the contribution of reflected electrons, described by the first term in (23), at a single interface of two semi-infinite parts.

Let us denote the spin-resolved values of the constant potential in the FM part as U_s ($s = \uparrow, \downarrow$) while the constant potential inside the NM part is set to zero. The reflection coefficients for electrons with a kinetic energy $E > 0$ in the NM part are given by

$$r_s(E) = \frac{1}{U_s}[2E - U_s - 2\sqrt{E(E-U_s)}], \qquad s = \uparrow, \downarrow, \tag{25}$$

where $\sqrt{E(E-U_s)} \equiv \mathrm{i}\sqrt{E(U_s-E)}$ for $E < U_s$. The electron motion in two directions parallel to the interface leads to the energy E varying between zero and the Fermi energy E_F ($E_F > 0$). The spin-mixing conductance then acquires a form

$$\frac{C_{\mathcal{L}}^{\mathrm{mix}}}{C_{\mathrm{Sh}}} = \frac{1}{E_F}\int_0^{E_F} [1 - r_\uparrow(E) r_\downarrow^*(E)]\,\mathrm{d}E, \tag{26}$$

where C_{Sh} is the Sharvin conductance of the NM metal (per spin channel); the energy integration in (26) corresponds to an integration over the $\mathbf{k}_\parallel$-vector. In order to make the model appropriate to the Cr/Co_2MnSi system (section 3.2), we identify the bottom of the spin-↓ band with the Fermi energy, $U_\downarrow \equiv E_F$, and study the spin-mixing conductance as a function of an attractive spin-↑ potential $U_\uparrow \equiv U < 0$.

An analysis of the model proves that the $r_s(E)$ (25) are real for $s = \uparrow$ and complex for $s = \downarrow$ (for energies $0 < E < E_F$), see figure 5(a), and they do not cause any destructive interference effects in the imaginary part of $C_{\mathcal{L}}^{\text{mix}}$ (26). The latter can thus reach non-negligible values with respect to the real part of $C_{\mathcal{L}}^{\text{mix}}$; see figure 5(b).

4. Conclusions

We have presented a formulation of the spin-mixing conductance of a thin ferromagnetic film attached to non-magnetic leads based on non-equilibrium Green's functions. We have implemented the derived formula in an *ab initio* technique and combined it with the coherent potential approximation. The first applications of the developed scheme revealed that the spin-mixing conductance of the Cu/Ni/Cu(111) system exhibits pronounced oscillations as a function of Ni thickness due to quantum-size effects and a weak exchange splitting of Ni. The spin-mixing conductance of the $Cr/Co_2MnSi/Cr(001)$ system possesses a surprisingly high imaginary part; this unusual feature can be understood on the basis of reflection coefficients in a free-electron model of an interface between a non-magnetic metal and a ferromagnetic half-metal.

Acknowledgments

The authors acknowledge the financial support provided by the Academy of Sciences of the Czech Republic (AV0Z20410507, KAN101630651, A100100616) and the Ministry of Education of the Czech Republic (MSM0021620834).

References

[1] Maekawa S and Shinjo T (ed) 2002 *Spin Dependent Transport in Magnetic Nanostructures* (Boca Raton, FL: CRC Press)
[2] Maekawa S (ed) 2006 *Concepts in Spin Electronics* (Oxford: Oxford University Press)
[3] Bass J and Pratt W P Jr 1999 *J. Magn. Magn. Mater.* **200** 274
[4] Slonczewski J C 1996 *J. Magn. Magn. Mater.* **159** L1
[5] Berger L 1996 *Phys. Rev.* B **54** 9353
[6] Katine J A, Albert F J, Buhrman R A, Myers E B and Ralph D C 2000 *Phys. Rev. Lett.* **84** 3149
[7] AlHajDarwish M, Kurt H, Urazhdin S, Fert A, Loloee R, Pratt W P Jr and Bass J 2004 *Phys. Rev. Lett.* **93** 157203
[8] Valet T and Fert A 1993 *Phys. Rev.* B **48** 7099
[9] Fert A, Cros V, George J-M, Grollier J, Jaffrès H, Hamzic A, Vaurès A, Faini G, Ben Youssef J and Le Gall H 2004 *J. Magn. Magn. Mater.* **272–276** 1706
[10] Barnas J, Fert A, Gmitra M, Weymann I and Dugaev V K 2005 *Phys. Rev.* B **72** 024426
[11] Barnas J, Fert A, Gmitra M, Weymann I and Dugaev V K 2006 *Mater. Sci. Eng.* B **126** 271
[12] Stiles M D and Zangwill A 2002 *Phys. Rev.* B **66** 014407
[13] Brataas A, Nazarov Y V and Bauer G E W 2000 *Phys. Rev. Lett.* **84** 2481
[14] Brataas A, Nazarov Y V and Bauer G E W 2001 *Eur. Phys. J.* B **22** 99
[15] Brataas A, Bauer G E W and Kelly P J 2006 *Phys. Rep.* **427** 157
[16] Xia K, Kelly P J, Bauer G E W, Brataas A and Turek I 2002 *Phys. Rev.* B **65** 220401
[17] Datta S 1995 *Electronic Transport in Mesoscopic Systems* (Cambridge: Cambridge University Press)
[18] Xia K, Zwierzycki M, Talanana M, Kelly P J and Bauer G E W 2006 *Phys. Rev.* B **73** 064420
[19] Zwierzycki M, Tserkovnyak Y, Kelly P J, Brataas A and Bauer G E W 2005 *Phys. Rev.* B **71** 064420
[20] Kovalev A A, Bauer G E W and Brataas A 2006 *Phys. Rev.* B **73** 054407
[21] Haug H and Jauho A-P 1996 *Quantum Kinetics in Transport and Optics of Semiconductors* (Berlin: Springer)
[22] Andersen O K and Jepsen O 1984 *Phys. Rev. Lett.* **53** 2571
[23] Turek I, Drchal V, Kudrnovský J, Šob M and Weinberger P 1997 *Electronic Structure of Disordered Alloys, Surfaces and Interfaces* (Boston, MA: Kluwer)
[24] Velický B 1969 *Phys. Rev.* **184** 614

[25] Kudrnovský J and Drchal V 1990 *Phys. Rev.* B **41** 7515
[26] Carva K, Turek I, Kudrnovský J and Bengone O 2006 *Phys. Rev.* B **73** 144421
[27] Waintal X, Myers E B, Brouwer P W and Ralph D C 2000 *Phys. Rev.* B **62** 12317
[28] Tserkovnyak Y, Brataas A and Bauer G E W 2002 *Phys. Rev. Lett.* **88** 117601
[29] Turek I, Kudrnovský J and Drchal V 2000 *Electronic Structure and Physical Properties of Solids* (*Springer Lecture Notes in Physics* vol 535) ed H Dreyssé (Berlin: Springer) p 349
[30] Kudrnovský J, Drchal V, Blaas C, Weinberger P, Turek I and Bruno P 2000 *Phys. Rev.* B **62** 15084
[31] Turek I, Kudrnovský J, Drchal V, Szunyogh L and Weinberger P 2002 *Phys. Rev.* B **65** 125101
[32] Drchal V, Kudrnovský J, Bruno P, Dederichs P H, Turek I and Weinberger P 2002 *Phys. Rev.* B **65** 214414
[33] Faleev S V, Léonard F, Stewart D A and van Schilfgaarde M 2005 *Phys. Rev.* B **71** 195422
[34] Wijn H P J (ed) 1991 *Magnetic Properties of Metals: d-Elements, Alloys and Compounds* (Berlin: Springer)
[35] Ishida S, Fujii S, Kashiwagi S and Asano S 1995 *J. Phys. Soc. Japan* **64** 2152
[36] Galanakis I, Dederichs P H and Papanikolaou N 2002 *Phys. Rev.* B **66** 174429
[37] Sakuraba Y, Miyakoshi T, Oogane M, Ando Y, Sakuma A, Miyazaki T and Kubota H 2006 *Appl. Phys. Lett.* **89** 052508